0026-895X/04/6605-1113–1122$20.00
MOLECULAR PHARMACOLOGY
Copyright © 2004 The American Society for Pharmacology and Experimental Therapeutics
Mol Pharmacol 66:1113–1122, 2004

Vol. 66, No. 5
1081/1179023
Printed in U.S.A.

An Investigation of the Neuroprotective Effects of Tetracycline Derivatives in Experimental Models of Retinal Cell Death

Darryl C. Baptiste, Andrew T. E. Hartwick, Christine A. B. Jollimore, William H. Baldridge, Gail M. Seigel, and Melanie E. M. Kelly

Retina and Optic Nerve Research Laboratory, Departments of Pharmacology (D.C.B., C.A.B.J., M.E.M.K.), Anatomy & Neurobiology (A.T.E.H., W.H.B.), and Ophthalmology & Visual Sciences (W.H.B., M.E.M.K.), Dalhousie University, Halifax, Nova Scotia, Canada; and Departments of Ophthalmology and Physiology and Biophysics, University at Buffalo, Buffalo, New York (G.M.S.)

Received April 2, 2004; accepted August 2, 2004

ABSTRACT

The purpose of this study was to determine the efficacy and putative mechanisms of action of tetracycline and minocycline in inhibiting retinal cell apoptosis after glutamate-induced excitotoxicity and trophic factor deprivation in a retinal cell line (E1A-NR.3) and in primary mixed retinal cell cultures. In addition, a differentiated PC-12 cell line was used to determine whether minocycline was neuroprotective after trophic withdrawal in a pure neuronal cell line devoid of glia. Results from this study demonstrated that minocycline, but not tetracycline, is protective in in vitro models of excitotoxicity-induced retinal cell apoptosis. Moreover, the protective effects provided by minocycline in retinal cells seemed independent of actions on *N*-methyl-D-aspartate receptors (NMDARs) and glutamate receptor-mediated Ca^{2+} influx. Doses of the NMDAR antagonist MK-801 (dizocilpine) and minocycline that alone provided no significant neuroprotection resulted in enhanced retinal cell survival when applied concurrently, suggestive of distinct signaling pathways, and minocycline was without effect on glutamate-induced Ca^{2+} influx, as assessed by calcium imaging. Minocycline was also neuroprotective after trophic factor withdrawal, producing a decrease in apoptosis and caspase-3 activation in both retinal cells and the PC-12 neuronal-like cell line. These results support a role for minocycline as a retinal neuroprotectant and demonstrate that the antiapoptotic actions of minocycline in retinal cells do not arise from the blockage of NMDARs or glutamate receptor-mediated Ca^{2+} influx but do involve inhibition of caspase-3 activation. In addition, the survival-promoting actions of minocycline may arise via actions on both neuronal and non-neuronal cell targets.

Compounds with neuroprotective properties are of considerable interest in the treatment of retinal neurodegenerative conditions such as glaucoma, where the potential exists to limit disease progression and preserve vision by promoting the survival of affected neurons (for review, see Weinreb and Levin, 1999). Glaucoma, a leading cause of vision loss and blindness, is characterized by the loss of retinal ganglion cells (RGCs). Although the exact cause of the development of damage is unclear, mechanical trauma, local ischemia and hypoxia, glutamate excitotoxicity, and the loss of trophic support may individually or collectively contribute to the death of RGCs (for review, see Quigley, 1999). In experimental animal models of glaucoma and RGC death, there is evidence that the loss of RGCs occurs through caspase-dependent apoptosis (Kermer et al., 1998; Tezel and Wax, 1999; McKinnon, 2003; Tahzib et al., 2004). In other neurodegenerative diseases, drugs that target key proteins involved in apoptotic cell signaling cascades have shown potential as neuroprotectants in experimental models (Larner, 2000; Friedlander, 2003; Liu and Hong, 2003), and several of these, including the glutamate receptor antagonist, memantine, and the glutamate release inhibitor riluzole, are now approved for clinical use in Alzheimer's disease (Reisberg et al., 2003) and amyotrophic lateral sclerosis (Lacomblez et al., 1996), respectively.

This work was supported by Canadian Institutes for Health Research (CIHR) grants IAO-13484 (to M.E.M.K) and MOP-15683 (to W.H.B.) and the CIHR Group grant in the Retina. D.C.B. was supported by a J. R. Johnston Studentship, and A.T.E.H. was supported by the CIHR/E. A. Baker Foundation and American Optometric Foundation Ezell Fellowships.

Article, publication date, and citation information can be found at http://molpharm.aspetjournals.org.

doi:10.1124/mol.104.001081.

ABBREVIATIONS: RGC, retinal ganglion cell; CNS, central nervous system; BDNF, brain-derived neurotrophic factor; CNTF, ciliary neurotrophic factor; NMDAR, *N*-methyl-D-aspartate receptor; DMEM, Dulbecco's modified Eagle's medium; FBS, fetal bovine serum; PBS, phosphate-buffered saline; NGF, nuclear growth factor; NA, numerical aperture; RT-PCR, reverse transcription-polymerase chain reaction; TBS, Tris-buffered saline; HBSS, Hanks' balanced salt solution; MK-801, dizocilpine; MPTP, 1-methyl-4-phenyl-1,2,5,6-tetrahydropyridine.

Minocycline is a highly lipophilic semisynthetic derivative of tetracycline that is capable of crossing the blood-brain barrier and exerting anti-inflammatory actions that are distinct from its ability to inhibit bacterial protein synthesis (Yrjänheikki et al., 1999). Minocycline is neuroprotective against glutamate excitotoxicity in primary CNS cultures, and the increase in neuronal survival was associated with inhibition of microglial activation and proapoptotic mediators (Tikka and Koistinaho, 2001; Tikka et al., 2001). In other experimental studies of neurodegeneration, minocycline has been reported to inhibit cytochrome *c* release from mitochondria as well as inhibit caspase-dependent and caspase-independent pathways of neuronal death (Zhu et al., 2002; Cao et al., 2003; Wang et al., 2003; Hughes et al., 2004; Scarabelli et al., 2004).

In the present study, we examined the neuroprotective abilities of minocycline and tetracycline in a rat retinal cell line and primary retinal cell cultures. This research had two objectives. First, we investigated whether these compounds could protect retinal cells in in vitro cell models of neuronal degeneration, namely glutamate excitotoxicity or trophic factor deprivation. Second, we attempted to better define the cellular targets involved in the antiapoptotic actions of the minocycline by determining whether the mechanism of the neuroprotection involves, at least in part, inhibition of NMDARs and associated Ca^{2+} influx and/or caspase-3 inhibition.

Materials and Methods

Materials. All culture reagents were obtained from Invitrogen (Carlsbad, CA) unless otherwise noted. Acridine orange and ethidium bromide dyes were purchased from Molecular Probes (Eugene, OR). RQ1 RNase-Free DNase and RNasin Ribonuclease Inhibitor were purchased from Promega (Madison, WI). One-Phor-All Buffer PLUS and pd$(T)_{12-18}$ [(poly)thymidine tail for reverse transcription] were purchased from Amersham Biosciences Inc. (Piscataway, NJ). First-strand cDNA buffer, dNTP Mix, and a recombinant *Taq* kit were purchased from MBI Fermentas (Burlington, ON, Canada). All other drug chemicals were obtained from Sigma-Aldrich (St. Louis, MO), except brain-derived neurotrophic factor (BDNF) and ciliary neurotrophic factor (CNTF) (both kindly provided by Regeneron Pharmaceuticals, Tarrytown, NY) and Zap-Oglobin (Beckman Coulter, Fullerton, CA). In all cases, L-glutamate was used but is referred to simply as glutamate.

Cell Cultures. We used a rat retinal precursor cell line, E1A-NR.3, derived from P6 rat retinal tissue immortalized by a replication-incompetent retrovirus containing the 12S portion of the E1A gene, which contains immortalizing but lacks transforming functions of the gene (Whyte et al., 1988). This cell line exhibits contact-inhibited and anchorage-dependent growth and is considered to be at the preglial/neuronal commitment stage, containing cells that express antigens specific for a number of different retinal phenotypes, including photoreceptors, bipolar cells, retinal ganglion cells, and retinal glial cells (Seigel, 1996; Seigel et al., 1998). The retinal precursor cell line expresses functional ionotropic NMDARs and non-NMDARs as well as GABA receptors (Sun et al., 2002) and has been used successfully for studies of retinal cell apoptosis in various experimental models of retinal cell death, including simulated ischemia, hypoxia, excitotoxicity, and serum withdrawal (Tezel and Wax, 1999; Seigel et al., 2000). E1A-NR.3 cells were seeded at an initial density of 1×10^5 cells/ml and maintained in growth media consisting of Dulbecco's modified Eagle's medium (DMEM) supplemented with 10% fetal bovine serum (FBS), 3% sodium bicarbonate, 1% each of L-glutamine, minimal essential medium nonessential amino acids, and vitamins, and 0.0125% gentamicin before experiments.

Primary retinal cultures, consisting of neurons and glial cells, were obtained from postnatal 6- to 10-day Long-Evans rats. All procedures were carried out in accordance with the Association for Research in Vision and Ophthalmology statement for the use of animals in ophthalmic and vision research. In brief, rat pups were anesthetized with halothane and decapitated. The eyes were enucleated, and posterior eyecups were placed in DMEM containing 1% gentamicin. The neural retinas were gently peeled off with fine forceps and incubated at 37°C in 1.25% trypsin for 5 min. FBS (10%) was added to end the trypsin reaction. Retinal cells were obtained after trituration through a narrow bore fire-polished Pasteur pipette, centrifugation at low speed for 3 min, aspiration of the supernatant, and resuspension in fresh growth medium (DMEM, 5% FBS, 1 ng/ml CNTF, 10 ng/ml BDNF, 1% N2 supplement, 1% gentamicin, and 100 μg/ml penicillin/streptomycin). The resulting cell suspension was seeded at a density of 2.5×10^5 cells/ml in culture dishes pretreated with poly-D-lysine (10 μg/ml) and laminin (2 μg/ml). Cultures were maintained at 37°C in a humidified atmosphere of 5% CO_2/95% air, and half of the growth medium was replaced every 2 to 3 days.

Culture and differentiation of PC-12 cells were carried out using established protocols (Greene, 1978). In brief, PC-12 cells maintained in media containing DMEM supplemented with 10% horse serum, 5% FBS, 2 mM L-glutamine, and 100 μg/ml penicillin/streptomycin and maintained at a cell density of 6×10^4/ml in 35-mm diameter culture dishes (BD Biosciences, Oakville, ON, Canada) precoated with rat-tail collagen (1 mg/ml). PC-12 cells were differentiated by adding 100 ng/ml nerve growth factor (7S NGF; Collaborative Research Inc., Bedford, MA). Differentiated cells were maintained for 7 days in a humidified atmosphere of 5% CO_2/95% O_2, and media were replenished every 2 to 3 days with fresh media.

Excitotoxic Cell Death Model. Glutamate-induced cell death was carried out in E1A-NR.3 cells and primary retinal cells at days 5 and 7 in vitro, respectively. The cell cultures, maintained in 24-well culture dishes, were divided into the following treatment groups: treatment media consisting of DMEM with Ham's F-12 nutrients (1:1 mixture), 10 mM $CaCl_2$, 5% FBS, 1% N2 supplement, 10 ng/ml BDNF, 1 ng/ml CNTF, and 1% gentamicin; treatment media with an additional 100 μM exogenous glutamate; and treatment media with an additional 100 μM glutamate and various concentrations of test drug. The formulation of DMEM/Ham's F-12 used for these experiments is known to enhance excitotoxicity, because it is Mg^{2+}-free and contains 30 μM glycine and 50 μM glutamate (Pellegrini and Lipton, 1993). This media formulation has been used previously for retinal excitotoxicity assays with additional increases in extracellular glutamate concentration (>100 μM), resulting in the selective death of retinal neurons with no significant effect on glia (Baptiste et al., 2002). In the present excitotoxicity assays, the final glutamate concentration for the treatment media with additional 100 μM exogenous glutamate was 150 μM. The transfer of the retinal cell line from growth media to treatment media resulted in no discernible decreases in cell survival; however, the transfer of primary retinal cultures to Mg^{2+}-free treatment media produced a small, but not significant, decrease in cell numbers (15–20%) compared with cell numbers in growth media. Therefore, in assays using primary retinal cell cultures, cell numbers in treatment medium were normalized with respect to cell numbers in growth media.

Trophic Withdrawal Cell Death Model. After 3 days in culture, primary and E1A-NR.3 rat retinal cells were gently washed three times with sterile phosphate-buffered saline (PBS) to remove trace amounts of growth medium containing trophic factors. The E1A-NR.3 retinal cell line cultures were divided into treatment groups consisting of treatment media containing 10% FBS, treatment media minus 10% FBS, treatment media minus 10% FBS, and various doses of minocycline (0.002–20 μM). Trophic factor-deprived primary rat retinal cell cultures had 5% FBS, CNTF (1 ng/ml), and BDNF (10 ng/ml) deleted from the media. Primary retinal cell and

E1A-NR.3 cultures were deprived of trophic factors for 24 and 48 h periods, respectively. NGF-differentiated PC-12 cell cultures were divided into treatment groups consisting of treatment media containing 10% horse serum, 5% FBS, and NGF (100 ng/ml); treatment media minus 10% horse serum, 5% FBS, and NGF (100 ng/ml); and various doses of minocycline (0.002–20 μM). NGF-differentiated PC-12 cell cultures were deprived of trophic support for a 24-h period.

Measurement of Cell Viability and Apoptosis. We used a cell lysis method (Baptiste et al., 2002) and acridine orange/ethidium bromide staining (Giuliano et al., 1998; Bertolesi et al., 2002) to determine viable and apoptotic cells in the glutamate excitotoxicity and trophic withdrawal models.

For the cell lysis assay, media and cells were removed from 24-well culture plates and placed into numbered test tubes for centrifugation. The supernatant was aspirated, and the resulting cell pellet of each well was resuspended in 200 μl of a 1:10 dilution of Zap-Oglobin detergent cell lysing solution. Viable, phase-bright nuclei, visible under inverted light microscopy, were quantified with a hemocytometer. Mean nuclei counts were obtained from 3 to 4 wells per treatment group and expressed as a percentage of viable nuclei in the media only group. Mean percentage data ± S.E.M. were obtained from 3 to 8 separate experiments. The drugs investigated were minocycline and tetracycline, and the effects of each drug were tested over a 3-log range (2–200 μM) in primary retinal cultures and a 4-log range (0.002–2 μM) in E1A-NR.3 cell lines, respectively.

For acridine orange and ethidium bromide staining, the media was removed, and cells were washed gently with PBS. After aspiration of the PBS, cells were treated with a mixture of acridine orange (100 μg/ml) and ethidium bromide (100 μg/ml) in PBS for 3 min. Cells were then visualized using fluorescence microscopy (Nikon Eclipse 800; Nikon, Mississauga, ON, Canada) with filters appropriate for fluorescein (Nikon B-2E; 450–490 nm excitation, 520–560 nm emission, 505 nm barrier). Images of the cells were captured with a Nikon FDX 35-mm digital camera through a Nikon Multi-Point Sensor System U-III using either Nikon 20× Plan Fluor (0.50 numerical aperture) or 100× Plan Fluor (1.30 numerical aperture) objectives. The number of viable (fluorescent green) and apoptotic (fluorescent orange with condensed, pyknotic nuclei) cells as a percentage of the total cells was calculated and analyzed after counting by a blinded observer.

Reverse Transcription-Polymerase Chain Reaction (RT-PCR). Total cellular RNA was obtained from E1A-NR.3 cells using TRIzol reagent according to the manufacturer's protocol. DNase I-treated RNA samples (2 μg) were used to generate single-stranded cDNA with Moloney murine leukemia virus reverse transcriptase after trophic factor withdrawal treatments. All PCR amplifications were carried out in a total volume of 25 μl with 2 ng of cDNA, 0.4 μM primers, 50 mM KCl, 10 mM Tris-HCL, pH 8.8, 1.5 mM $MgCl_2$, 0.2 mM dNTP, and 2.5 units of recombinant *Taq* polymerase. Primer sequences have been published previously for caspase-3 (Harrison et al., 2001) and cyclophilin (Hirooka et al., 2002). To compare mRNA expression levels between treated and untreated cells, the number of PCR cycles was first determined to be in the linear range. The number of cycles and annealing temperatures for each gene investigated were 20 cycles at 50°C for cyclophilin and 30 cycles at 55°C for caspase-3. The PCR products were resolved by staining with ethidium bromide and electrophoresis in 1.5% agarose gels. Results were visualized under UV illumination using a Gel Doc apparatus (Bio-Rad, Mississauga, ON, Canada). Images of the PCR bands were analyzed semiquantitatively using Molecular Analyst image analysis software version 1.5 (Bio-Rad).

Western Blotting. E1A-NR.3 cells were washed with PBS and transferred to a 1.5-ml tube and centrifuged at 5000 rpm for 1 min at 4°C. The cells were resuspended in 100 μl of cell lysis buffer (Cell Signaling Technology Inc., Beverly, MA), incubated on ice for 20 min, and then centrifuged for 15 min at 13000 rpm at 4°C. The resulting supernatant was transferred to a fresh 1.5-ml tube, and the protein concentration was determined using the bicinchoninic acid protein assay kit (Pierce, Rockford, IL) with bovine serum albumin as a calibration standard. Protein samples were then diluted to equivalent concentrations with aliquots of SDS buffer and heated at 95°C for 5 min. Proteins were separated by SDS-polyacrylamide gel electrophoresis (12%). Proteins were electrotransferred to a nitrocellulose membrane at 95 V for 1 h. The membranes were dried for 2 h, incubated first in blocking buffer (0.1% Tween 20 with 5% nonfat dry milk in Tris-buffered saline; TBS) for 2 h, and then incubated with a 1:1000 dilution (in blocking buffer) of cleaved caspase-3 antibody (rabbit, Asp175; Cell Signaling Technology) overnight at 4°C on an orbital shaker. Membranes were then washed three times with TBS-Tween 20 for 10 min before the application of horseradish peroxidase-conjugated goat anti-rabbit IgG secondary antibody (Vector Laboratories, Burlington, ON, Canada) at room temperature on an orbital shaker for 1 h. After this, membranes were washed three times with TBS-Tween 20 at room temperature on the orbital shaker for 20 min. Protein bands were visualized with the enhanced chemiluminescence detection system (ECL System; Amersham Biosciences Inc.) and exposed to film (Hyperfilm ECL; Amersham Biosciences Inc.).

Calcium Imaging. Calcium imaging experiments were performed on primary mixed retinal cell cultures consisting of neurons and glia that had survived 6 to 7 days in vitro. The cells were incubated in 5 μM Fura-2/acetoxymethyl ester (Molecular Probes) dissolved in a modified Mg^{2+}-free Hanks' balanced salt solution (HBSS; 2.6 mM $CaCl_2$, 15 mM HEPES, pH 7.4) for 30 min in the dark at 37°C. The Fura-2/acetoxymethyl ester was first dissolved in dimethyl sulfoxide (0.1% final concentration in HBSS) and then solubilized in HBSS containing 0.1% pluronic acid F-127 (Molecular Probes).

The coverslip-plated retinal cells loaded with Fura-2 were then transferred to a microscope chamber that was constantly superfused with the Mg^{2+}-free HBSS at 34 to 36°C and bubbled with 100% oxygen. The calcium imaging rig, consisting of a cooled charged-coupled device camera fitted to a microscope with a water-immersion objective (numerical aperture, 0.8 W; Achroplan 40×; Carl Zeiss, Thornwood, NY), has been described in detail elsewhere (Baptiste et al., 2002). Fura-2 fluorescence was produced by excitation from a 75-W Xenon lamp (Ludl Electronic Products, Hawthorne, NY) and appropriate filters (XF04 set; excitation, 340 or 380 nm; emission, 510 nm; dichroic, >430 nm) (Omega Optical Inc., Brattleboro, VT). Ratiometric (340 nm/380 nm) images were generated by an imaging system (Imaging Workbench 2.2; Axon Instruments, Union City, CA) and saved to the hard disk of a computer. The background fluorescence was measured and subtracted from each image. The mean Fura-2 ratio for each cell was calculated over a large area of the cell soma, well separated from the edge of the cell.

All treatment solutions were dissolved in the Mg^{2+}-free HBSS and delivered to the chamber by a peristaltic pump (Gilson Medical Electronics, Middleton, WI) at a rate of approximately 1 ml/min. The Fura-2 ratio, indicative of the free intracellular calcium levels ($[Ca^{2+}]_i$), was elevated in the isolated neurons by the application of a short pulse (30 s) of 100 μM glutamate. Glycine (100 μM), a coagonist of glutamate at the NMDARs, was added to the glutamate solution to enhance potential NMDAR activation (Johnson and Ascher, 1987). During treatments, image pairs were collected as often as every 3 s, but to limit photodamage, images were collected less frequently (20 s) during intervening periods.

Statistical Analysis. Unless otherwise noted, data were analyzed by repeated measures analysis of variance followed by Dunnett's multiple comparison test. The criterion for significance was set at $p < 0.05$.

Results

Effects of Tetracycline Derivatives on Glutamate-Induced Retinal Cell Death. Figure 1 shows data from

experiments studying the survival of E1A-NR.3 retinal cell cultures in treatment media containing 100 μM additional glutamate alone or in combination with various concentrations (0.002–2 μM) of tetracycline or minocycline. Tetracycline failed ($p > 0.05$, $n = 3$) to increase the survival of retinal cell line cultures at all concentrations tested (0.002–2 μM) compared with that observed in the glutamate-only treated group (Fig. 1A). In contrast, minocycline produced a dose-dependent increase in viable E1A-NR.3 cells at concentrations between 0.002 to 0.2 μM (Fig. 1B). Viable cell numbers (mean ± S.E.M.) in the presence of 0.002, 0.02, 0.2, and 2 μM minocycline were 77 ± 5, 83 ± 6, 85 ± 5, and 67 ± 7% of the control media-only group compared with 60 ± 5% of the control in the glutamate-only group ($n = 4$). This increase in cell viability was significant at 0.02 and 0.2 μM minocycline ($p < 0.05$ and $p < 0.01$, respectively), with a diminished effect at higher concentrations of minocycline (2 μM, $p > 0.05$).

A similar dose-dependent increase in cell survival was produced by minocycline in primary retinal cell cultures exposed to 100 μM additional glutamate (Fig. 2). Viable primary retinal cell numbers in the presence of 2, 20, and 200 μM minocycline in the treatment media were 99 ± 11, 120 ± 18, and 115 ± 11% compared with 56 ± 4% for cells in the glutamate-only group ($n = 3$). Increases in cell survival were significant at all concentrations tested ($p < 0.05$, $p < 0.01$, and $p < 0.01$ for 2, 20, and 200 μM minocycline, respectively). At concentrations below 2 μM, minocycline was not effective in increasing cell survival in all primary retinal cultures tested ($n = 2$, data not shown). As an internal control, minocycline (20 μM) was added to wells receiving treatment media only. Cell viability for this group was not significantly different (117 ± 19%, $p > 0.5$, $n = 4$) from the control treatment media-only group.

Drugs that block NMDARs or alter glutamate-induced increases in $[Ca^{2+}]_i$ have been shown to increase retinal cell viability after excitotoxic insult (Pellegrini and Lipton, 1993; Osborne et al., 1999; Baptiste et al., 2002). To determine whether the neuroprotective actions of minocycline in retinal cell cultures may occur, in part, via actions on NMDARs, we examined whether the cell survival observed with minocycline was additive or synergistic with the selective noncompetitive NMDAR antagonist MK-801 (dizocilpine). If common mechanisms or pathways of inhibition underlie the actions of both of these classes of drugs, then the effects should be additive, and the survival-promoting effects of both drugs should be close to the sum of that measured with either drug alone. In contrast, if the effects of combined treatments are much greater than that expected from the sum of either treatment alone, this suggests that the drugs may act by synergistic pathways that are largely independent.

We first established the doses of MK-801 that produced increased cell survival in retinal cell cultures to determine a

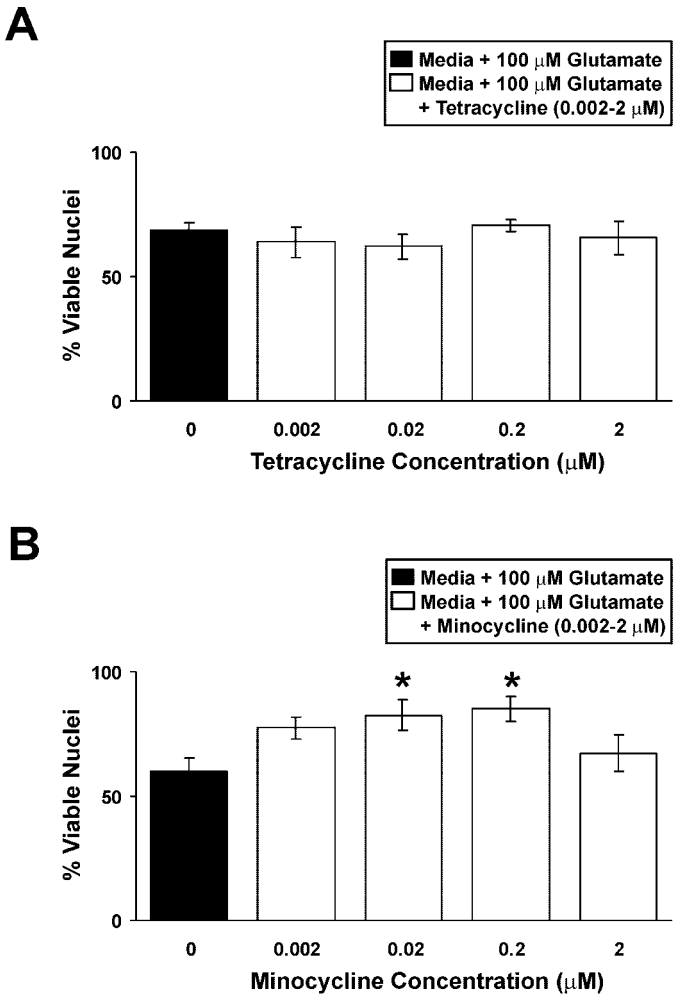

Fig. 1. Effect of tetracycline and minocycline on glutamate-induced E1A-NR.3 retinal cell death. Percentage of survival of the E1A-NR.3 rat retinal cell line cultures treated with tetracycline ($n = 3$) (A) or minocycline ($n = 4$) (B) after 24 h of glutamate excitotoxicity. Viable cells were assessed by counting the density of intact nuclei after Zap-Oglobin cell lysis. Treatment groups consisted of the following: media containing DMEM/Ham's F-12 formulation; media plus an additional 100 μM glutamate; and media and glutamate plus various doses of the tetracycline or minocycline (0.002–2 μM). Data are expressed as the mean ± S.E.M. percentage of survival relative to the media-only control group. *, $p < 0.05$ and **, $p < 0.01$ compared with the media plus glutamate group.

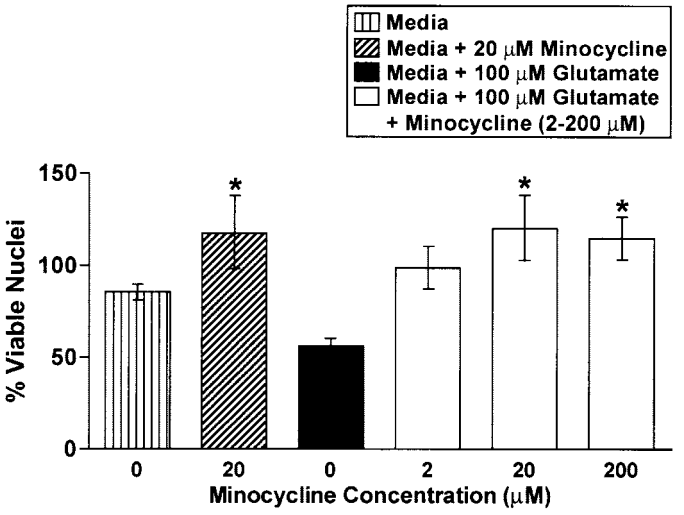

Fig. 2. Effect of minocycline on glutamate-induced primary retinal cell death. Percentage of survival of primary mixed rat retinal cell cultures treated with minocycline after 24 h of glutamate excitotoxicity. Viable cells were assessed by counting the density of intact nuclei after Zap-Oglobin cell lysis. Treatment groups consisted of the following: media containing DMEM/Ham's F-12 formulation; media plus an additional 100 μM glutamate; and media and glutamate plus various doses of minocycline (2–200 μM). Data are from three separate experiments and are expressed as the mean ± S.E.M. percentage of survival relative to the media-only control group. *, $p < 0.05$ and **, $p < 0.01$ compared with the media plus glutamate group.

submaximal or threshold dose for neuroprotection. Figure 3A shows data from experiments studying the survival of E1A-NR.3 retinal cell cultures in treatment media containing glutamate, both alone and in combination with increasing concentrations (1–100 μM) of the NMDAR antagonist MK-801. A dose-dependent increase in E1A-NR.3 survival was seen with MK-801; mean cell survival for six separate experiments increased from 60 ± 4% for the glutamate-only group to 71 ± 11, 85 ± 8 ($p < 0.05$), and 103 ± 9% ($p < 0.01$) of the untreated control group with 1, 10, and 100 μM MK-801, respectively.

Figure 3B shows the results of three experiments in which submaximal concentrations of MK-801 (1 μM) and minocycline (0.002 μM) that failed to show significant protection in excitotoxicity assays with E1A-NR.3 cultures were tested separately and in combination. In the glutamate-only group, cell viability was reduced to 68 ± 4% of control. On their own, neither 1 μM MK-801 nor 0.002 μM minocycline significantly protected retinal cells from excitotoxic death (72 ± 7 and 68 ± 3%, respectively, compared with the glutamate-only group). On the other hand, the combination of submaximal doses of MK-801 and minocycline produced a significant increase in viability (99 ± 6%, $p < 0.01$) compared with the glutamate-only group. The enhanced cell viability seen with the combination of submaximal doses of MK-801 and minocycline was significantly greater than groups receiving either drug alone ($p < 0.01$). The effect of combined treatment with 0.002 μM minocycline and 1 μM MK-801 produced a neuroprotective effect that was comparable with 100 μM MK-801 (Fig. 2) and exceeded the effect of the maximum dose (0.2 μM) of minocycline (Fig. 1B). It is clear, therefore, that the combined treatment was synergistic, enhancing the effect so that it exceeded what would be expected from a simple additive effect of this dose of either drug alone. This suggests that the effect of minocycline is in large part independent of an action at NMDARs, the site of action of MK-801, although it does not exclude actions of minocycline at targets downstream of NMDARs in addition to the activation of concurrent NMDAR-independent signaling pathways.

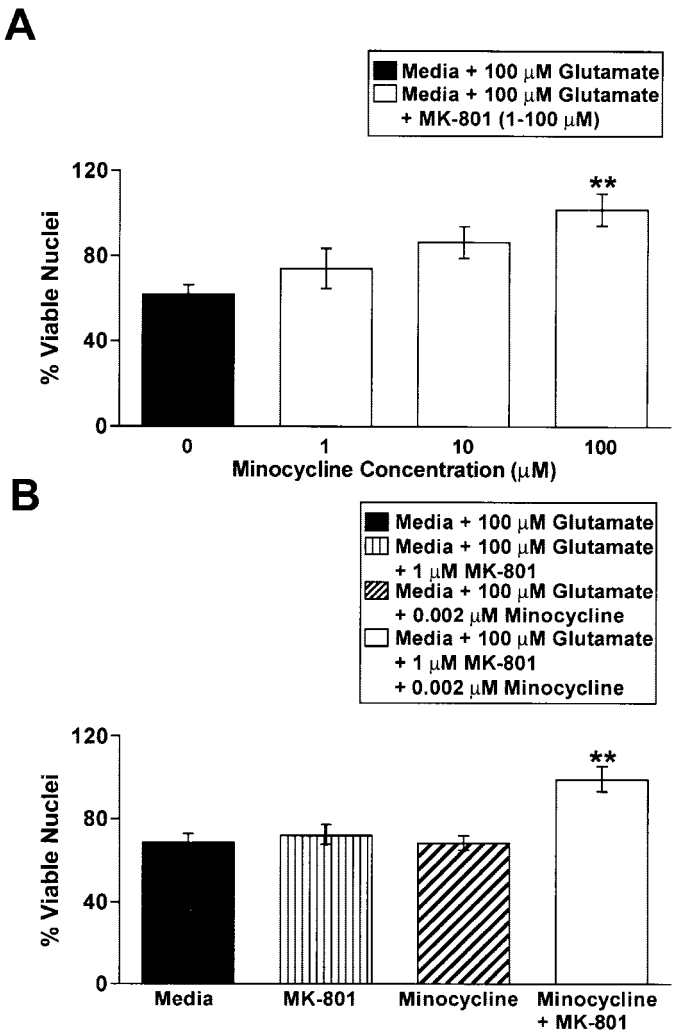

Fig. 3. Effect of MK-801 and minocycline on E1A-NR.3 retinal cell viability after exposure to excitotoxic media. Percentage of survival of the E1A-NR.3 rat retinal cell line cultures treated with the NMDAR blocker MK-801 (1–100 μM) alone ($n = 6$) (A) or the combination of submaximal doses of MK-801 (1 μM) with minocycline (0.002 μM) ($n = 3$) (B) after 24 h of glutamate excitotoxicity. Viable cells were assessed by counting the density of intact nuclei after Zap-Oglobin cell lysis. Treatment groups consisted of the following: media containing DMEM/Ham's F-12 formulation; media plus an additional 100 μM glutamate; and media and glutamate plus various doses of the drug. Data represent the mean ± S.E.M. *, $p < 0.05$ and **, $p < 0.01$ compared with the media plus glutamate group.

To further confirm that the neuroprotective effects of minocycline were independent of actions at glutamate receptors, we used Ca^{2+} imaging to determine the effects of minocycline on glutamate-induced increases of $[Ca^{2+}]_i$ in cultured primary retinal neurons. Figure 4A illustrates the effect of minocycline on glutamate-induced $[Ca^{2+}]_i$ increase in a representative retinal neuron. Glutamate (100 μM) increased the Fura-2 fluorescence ratio from a resting level of approximately 0.50 to a peak of approximately 0.85 during a 4.5-s exposure of 100 μM glutamate (+100 μM glycine). A second application of glutamate in the presence of 1 μM minocycline did not affect the response (peak ratio) to glutamate, and the magnitude of the response to glutamate was maintained after washout of minocycline. Similar results (Fig. 4B) were found in all the retinal neurons studied ($n = 13$).

Effects of Minocycline on Trophic Withdrawal-Induced Apoptosis in Retinal Cells. Because the neuroprotective effects of minocycline seemed independent of glutamate-receptor mediated Ca^{2+} influx in retinal models of excitotoxicity, further experiments examined whether minocycline was neuroprotective in a serum and trophic factor withdrawal model of cell death in E1A-NR.3 cells and primary retinal cell cultures, respectively. Figure 5 shows the results of a cell viability assay with acridine orange and ethidium bromide carried out with E1A-NR.3 cells maintained in serum-containing media for 48 h and cells deprived of serum for 48 h in the absence or presence of minocycline. E1A-NR.3 cells maintained in serum-containing media (media + serum) take up acridine orange to display green viable nuclei (Fig. 5A). On the other hand, E1A-NR.3 maintained in serum-free media (media − serum) incorporated both acridine orange and ethidium bromide within cellular DNA to display an increased population of pyknotic orange/red nuclei that are characteristic of cells undergoing apoptosis (Fig. 5B). Upon adding 0.02 or 0.2 μM minocycline to cells lacking serum (media − serum + minocycline) (Fig. 5, C and D, respectively), an increased density of viable nuclei were observed. The percentage of pyknotic nuclei (mean ± S.E.M., $n = 3$) was 15 ± 3, 39 ± 2, 16 ± 4, and 21 ± 3% for cells

cultured in serum-containing media, serum-free media, and serum-free media plus 0.02 and 0.2 μM minocycline, respectively (Fig. 5E). The decreases in pyknotic nuclei observed were significant for cells receiving serum-containing media ($p < 0.01$) as well as for serum-deprived retinal cells supplemented with either dose of minocycline ($p < 0.01$) compared with the cells receiving just serum-free media.

Similar results were also obtained using primary retinal cell cultures deprived of trophic support (Fig. 6). Cell viability assays demonstrated that the exposure of primary retinal cultures to serum and trophic factor-free media for 24 h reduced viable cells to 52 $\pm$ 5% ($n = 3$) compared with primary cell cultures receiving serum and trophic factor support. In trophic factor-deprived primary retinal cultures supplemented with increasing minocycline concentrations of 0.002, 0.02, 0.2, 2, and 20 μM, cell viability was increased to 54 $\pm$ 4, 53 $\pm$ 1, 66 $\pm$ 4, 78 $\pm$ 10, and 61 $\pm$ 8%, respectively ($n = 3$). The increase in viability noted at 2 μM minocycline was significant ($p < 0.05$) compared with control. The addition of 20 μM minocycline to control media containing trophic factors did not result in a significant increase in the number of viable cells compared with control ($p > 0.05$, $n = 3$) but was significantly increased compared with trophic factor-deprived cultures in the absence of minocycline ($p < 0.01$, $n = 3$).

Effect of Minocycline on Caspase-3 Expression in Retinal Cells after Serum Withdrawal. Previous studies in different experimental models have indicated that the neuroprotective properties of minocycline may be attributed in part to inhibition of caspase activation (Chen et al., 2000; Zhu et al., 2002). Furthermore, several studies in E1A-NR.3 retinal cells have indicated that apoptosis in these cells after simulated ischemia, excitotoxicity, and serum deprivation include a proteolysis cascade involving caspase-3 (Tezel and Wax, 1999; Barber et al., 2001). We therefore examined whether the neuroprotective actions of minocycline in retinal

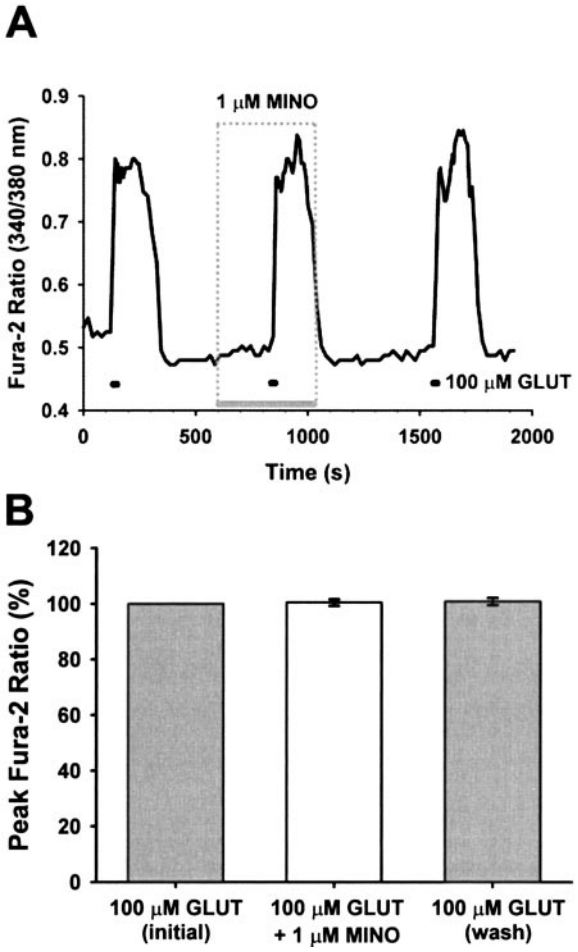

Fig. 4. Effect of minocycline on glutamate-induced calcium influx in isolated retinal neurons. Minocycline does not affect glutamate-induced calcium influx in isolated retinal neurons. A, example trace from an individual retinal neuron illustrating that the increase in the Fura-2 fluorescence ratio induced by 100 μM glutamate (GLUT) was the same whether 1 μM minocycline (MINO) was present or absent. B, mean data ($n = 13$) for calcium imaging experiments, normalized to the initial glutamate response.

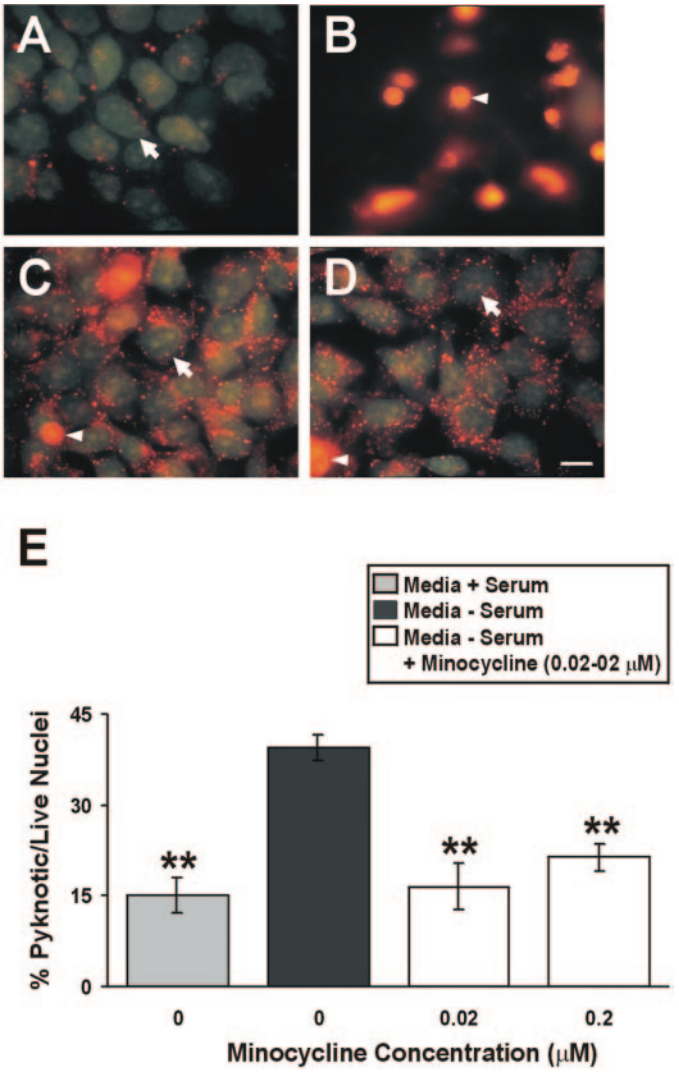

Fig. 5. Effect of minocycline treatment on serum withdrawal-induced apoptosis in E1A-NR.3 retinal cells. Cell viability assay was assessed 48 h later with acridine orange and ethidium bromide dye exclusion in E1A-NR.3 cells treated with growth media containing serum (A), no serum (B), no serum plus 0.02 μM (C), or 0.2 μM minocycline (D). Viable nuclei with acridine orange incorporation stain green (arrows), whereas dead cells have both acridine orange and ethidium bromide intercalated within genomic DNA to display orange/red pyknotic nuclei characteristic of apoptosis (arrowheads in A–D). E, histogram of the percentage of pyknotic nuclei observed from five high-powered fields (area = 0.23 mm^2) per treatment group in three separate experiments. **, $p < 0.01$ compared with the no serum group.

cell cultures after serum deprivation was associated with alterations in caspase-3 activation. We used RT-PCR to examine caspase-3 mRNA expression in cultures of E1A-NR.3 retinal cells incubated for 18 h with either media containing serum, serum-free media, or serum-free media plus 0.02 or 0.2 μM minocycline. Figure 7A shows PCR products obtained using primers specific for caspase-3 and cyclophilin, visualized by UV fluorescence after gel electrophoresis. Increased caspase-3 mRNA expression was seen for E1A-NR.3 cells maintained in serum-free media for 18 h, consistent with caspase-3 dependent apoptosis in retinal cells previously reported after serum withdrawal (Barber et al., 2001). Although a decrease in caspase-3 mRNA was not seen for serum-free cells treated with 0.02 μM minocycline (lane 3), caspase-3 was reduced in serum-free cells treated with 0.2 μM minocycline (lane 4). Figure 7B shows densitometry results of caspase-3 mRNA, normalized to cyclophilin, from three separate experiments in which E1A-NR.3 cells were grown for 18 h in serum-containing media, serum-free media only, and serum-free media with 0.02, 0.2, or 2.0 μM minocycline. Densitometry values of caspase-3, relative to cyclophilin, for serum-containing, serum-free, and serum-free plus 0.02 and 0.2 μM minocycline were 26 $\pm$ 8, 48 $\pm$ 11, 57 $\pm$ 22, and 19 $\pm$ 7%, respectively.

The effect of minocycline on caspase-3 protein expression was also examined in serum-free E1A-NR.3 cells using Western blotting. The presence of caspase-3 activation was assessed via the expression of the 17- and 19-kDa subunits that were derived from the proteolytic cleavage of the 32-kDa proenzyme caspase-3. As shown in Fig. 7C, serum withdrawal increased caspase-3 activation, but this increase was reduced after a 48-h incubation with minocycline at 0.2 and 2.0 μM. Densitometry of the 19-kDa band showed a 286% (n = 2) increase when serum was absent. Minocycline at both 0.2 (n = 2) and 2.0 μM (n = 1) reduced the density of the 19-kDa band by about 15% relative to the density under serum-free conditions. However, consistent with our RT-PCR results, lower doses of minocycline (0.02 μM) did not decrease the density of cleaved caspase-3 (n = 2) after serum withdrawal.

Because E1A-NR.3 retinal cells and primary retinal cultures represent a mixed cell population of retinal neurons and glia, we also tested the effects of minocycline on NGF-differentiated PC-12 cells, a well established model for neuronal neuroprotection studies (for example, see Boniece and Wagner, 1993; Wirtz-Brugger and Giovanni, 2000; Weinreb et al., 2004), to confirm whether minocycline could exert neuroprotective effects by targeting neurons directly in the absence of glia (Fig. 8). Once differentiated to a pure neuro-

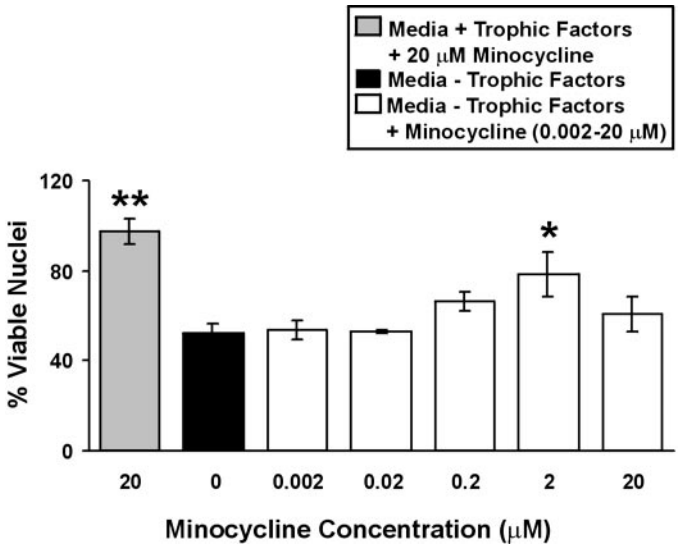

Fig. 6. Effect of minocycline treatment on trophic factor deprivation-induced primary retinal cell death. Percentage of survival of primary mixed rat retinal cell cultures treated with minocycline after a 24-h exposure to media without trophic factors. Viable cells were assessed by counting the density of intact nuclei after Zap-Oglobin cell lysis. Treatment groups consisted of media + trophic factors, media − trophic factors, or media − trophic factors + minocycline (0.002–20 μM). Data are from three separate experiments and are expressed as the mean $\pm$ S.E.M. of the media + trophic factor control group (100%). *, $p < 0.05$ and **, $p < 0.01$ compared with the no serum group.

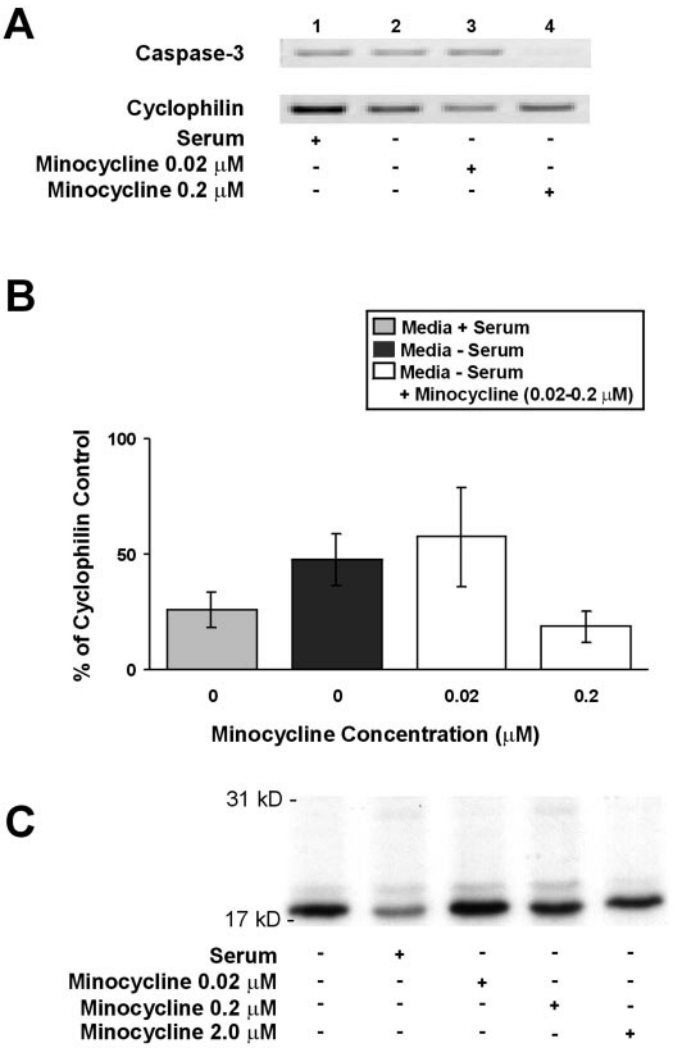

Fig. 7. Effect of minocycline on caspase-3 expression after trophic factor deprivation. A, electrophoresis of RT-PCR products for caspase-3 (646 base pairs) and cyclophilin (371 base pairs) after an 18-h incubation in growth media containing trophic factors (lane 1), no trophic factors (lane 2), and no trophic factors but supplemented with 0.02 (lane 3) and 0.2 μM (lane 4) minocycline. (n = 3). B, results of caspase-3 ratio of PCR products to that of cyclophilin densitometry. Data represent the mean $\pm$ S.E.M. ratio. C, Western blot results using antibodies specific for cleaved 17- and 19-kDa caspase-3 subunits in E1A-NR.3 cells after a 48-h incubation in media containing no trophic factors (lane 1), trophic factors (lane 2), no trophic factors but supplemented with 0.02 μM (lane 3), and 0.2 (lane 4) or 2.0 μM (lane 5) minocycline.

nal phenotype, trophic factor-starved PC-12 cells cannot dedifferentiate by re-entering the cell cycle and are committed to apoptosis (Lambeng et al., 1999). PC-12 cell cultures were cultured in the presence or absence of serum and NGF for 24 h. PC-12 cells maintained in the presence of serum and trophic factors extended neurites (Fig. 8A) and incorporate acridine orange within cellular DNA to demonstrate viable green nuclei (Fig. 8, B and C). The removal of trophic support resulted in the degeneration of neuronal processes (Fig. 8D), and the resulting acridine orange and ethidium bromide DNA incorporation revealed an increased generation of orange/red pyknotic nuclei (Fig. 8, E and F). PC-12 cells treated with 0.02 μM minocycline after trophic factor withdrawal showed increased neurite numbers (Fig. 8G) and decreased numbers of apoptotic nuclei (Fig. 8, H and I). Figure 8J shows that increasing minocycline concentrations (0.002–20 μM) produce a dose-dependent decrease in the number of apoptotic nuclei up to 0.2 μM minocycline. The proportion of pyknotic nuclei for differentiated PC-12 cells in the presence, absence, and absence of trophic support plus minocycline (0.002, 0.02, 0.2, 2, and 20 μM) in three separate experiments was 1 ± 0, 48 ± 4, 43 ± 6, 29 ± 3, 26 ± 4, 26 ± 2, and 34 ± 4%, respectively. The reduction in the pyknotic/live nuclei ratio for the 0.02 to 2 μM minocycline and 20 μM minocycline treatment groups was significant at $p < 0.01$ and $p < 0.05$, respectively.

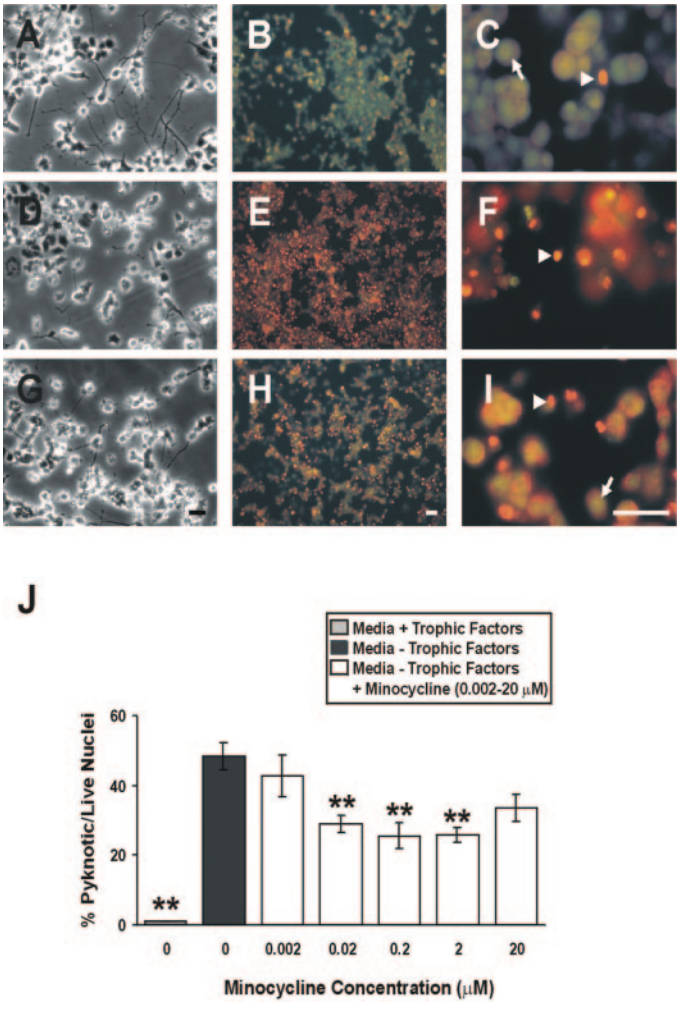

Fig. 8. Effect of minocycline treatment on trophic factor deprivation-induced apoptosis in NGF-differentiated PC-12 cells. Cell viability assessed 24 h later with acridine orange/ethidium bromide (acridine orange/ethidium bromide) dye exclusion in NGF-differentiated PC-12 cell cultures treated with growth media containing serum and NGF (B and C), no serum or NGF (E and F), and no serum or NGF plus 0.02 μM minocycline (H and I). Viable nuclei with acridine orange incorporation stain green (arrows in C and I), whereas dead cells have both acridine orange and ethidium bromide intercalate within genomic DNA to display orange/red pyknotic nuclei characteristic of apoptosis (arrowheads in C, F, and I). The effect of trophic factor deprivation on PC-12 neuronal processes can be seen in the phase photomicrographs (A, D, and G). J, histogram of the ratio of pyknotic-to-live nuclei obtained from five high-powered fields (area = 0.23 mm^2) per treatment group in three separate experiments. **, $p < 0.01$ compared with the no serum or NGF group.

Discussion

This work compared the neuroprotective actions of the tetracycline derivatives minocycline and tetracycline in in vitro retinal cell models of apoptosis (excitotoxicity and trophic withdrawal). We used an immortalized retinal cell line, E1A-NR.3, and mixed primary retinal cultures. A major finding of this study was that minocycline, but not tetracycline, was able to prevent excitotoxic death of cultured retinal cells. Our previous studies have demonstrated that the cell death seen after glutamate excitotoxicity in primary retinal cultures results from the loss of neurons and not glia (Baptiste et al., 2002), supporting a neuroprotective action of minocycline for retinal neurons. Our present findings demonstrate that minocycline is neuroprotective, regardless of whether excitotoxic stress or serum or trophic factor withdrawal induced retinal neuron apoptosis. The neuroprotective actions of minocycline in retinal cells involving, in part, inhibition of caspase-3, were independent of NMDAR inhibition and did not arise via a reduction in glutamate receptor-induced Ca^{2+} influx.

In other studies in primary spinal cord cultures (Tikka and Koistinaho, 2001) and cultured cortical neurons (Zhu et al., 2002), minocycline has also been reported to provide neuroprotection against *N*-methyl-D-aspartate neurotoxicity. The actions of minocycline in these studies included inhibition of proliferating microglial cells and *N*-methyl-D-aspartate-induced activation of p38 mitogen-activated protein kinase, inhibition of caspase-1, caspase-3, and the inducible form of nitric-oxide synthase and a decrease in mitochondrial permeability transition-mediated cytochrome *c* release. Although the actions of minocycline on different cellular targets still remain to be clarified, it is likely that the multifaceted actions of this tetracycline derivative may arise from actions at multiple targets, involving both direct actions on neurons as well as on microglia. For example, in our study, minocycline was neuroprotective in mixed retinal cell cultures composed of neurons and glia but was also able to protect differentiated PC-12 cells from apoptosis after trophic withdrawal. Both caspase-3 (Vaghefi et al., 2004) and mitogen-activated protein kinase (Lambeng et al., 2003) apoptotic pathways are activated in NGF-deprived PC-12 cells. In our trophic factor withdrawal experiments using differentiated PC-12 cells, minocycline maintained PC-12 neuronal-like processes and prevented morphological nuclear condensation, confirming that the neuroprotective actions of minocycline are not confined to inhibition of microglia or secondary to the release of glial-derived trophic factors but can arise from direct actions on neuronal targets.

In other experimental studies using mouse models of amyotrophic lateral sclerosis (Kriz et al., 2002) and Parkinson's disease (Liberatore et al., 1999; Wu et al., 2002), minocycline was found to effectively inhibit activated microglia with minimal effects on astrocytes. However, the neuroprotective effects of minocycline seen in the 1-methyl-4-phenyl-1,2,5,6-tetrahydropyridine (MPTP) Parkinson's mouse model seemed to exceed the beneficial effects that would be expected by microglial-derived inducible nitric-oxide synthase inhibition, implying an additional direct protective effect of minocycline on neurons and/or inhibition of other microglial-associated cytotoxins (Wu et al., 2002). In contrast, a more recent study using a different dosing regimen found that although minocycline blocked MPTP-induced microglial activation, MPTP toxicity to dopaminergic neurons was exacerbated by minocycline (Yang et al., 2003).

Unlike minocycline, our results indicated that tetracycline did not significantly affect cell survival in retinal cell cultures. Previous experimental studies of brain ischemia have demonstrated that minocycline is significantly more lipid-soluble than tetracycline and is able to effectively cross the blood-brain barrier to distribute throughout the CNS, including the retina, producing a reduction in ischemic neuronal damage (Yrjänheikki et al., 1998, 1999). The lack of effect of tetracycline in this and other studies has been attributed to the poor tissue distribution of this drug to the CNS. Our results in the E1A-NR.3 retinal cell cultures indicate that, despite adequate drug concentrations at cellular targets, tetracycline is still markedly less efficacious than minocycline and produced no significant neuroprotection. Therefore, the neuroprotective efficacy of minocycline, compared with tetracycline, may be the result of more than tissue penetration, suggesting that its neuroprotective property may not be a feature shared by all other members of the tetracycline family of molecules.

On average, the optimal neuroprotective concentrations for minocycline in the retinal cell line were different from the primary retinal cultures, probably because the cell line is more homogenous and consistent in that the numbers of the different cell phenotypes present is relatively constant from culture to culture under the conditions used. In contrast, in the primary cultures there is much more heterogeneity leading to more variability in the net response to neuroprotectants.

Our results also demonstrated that the neuroprotective actions of minocycline in retinal cultures do not result from inhibition of NMDARs or glutamate-receptor induced increases in Ca^{2+} influx, because the NMDAR blocker MK-801 and minocycline together produced supra-additive survival at submaximal doses, suggestive of distinct signaling pathways, and because minocycline had no significant effects on glutamate-induced Ca^{2+} influx in retinal neurons. This result is consistent with the finding that combined treatment with MK-801 and the nonselective caspase inhibitor *N*-benzyloxycarbonyl-VAD-fluoromethyl ketone results in synergistic neuroprotection in an in vivo rat model of cerebral hypoxia/ischemia (Schulz et al., 1998) and the finding that minocycline was not able to inhibit Ca^2-mediated loss of mitochondrial membrane potential (Zhu et al., 2002).

Minocycline neuroprotection probably involves inhibition of caspase-mediated cell death (Friedlander, 2003; Wang et al., 2003; Hughes et al., 2004; Scarabelli et al., 2004). An investigation of caspase-3 activation in E1A-NR.3 cells after serum withdrawal indicated that minocycline can inhibit caspase-3 activation in retinal cells. Previous studies using the E1A-NR.3 retinal cell line or R28 cells, which are a subclone of E1A-NR.3, demonstrated that excitotoxicity and serum withdrawal-induced apoptosis involved activation of caspase-3 (Tezel and Wax, 1999; Barber et al., 2001). In R28 cells, the activation of caspase-3 after serum withdrawal was mediated through the phosphatidylinositol 3-kinase/Akt pathway. However, although our results support caspase-3-dependent mechanisms of apoptosis in E1A-NR.3 cells, the concentration of minocycline that was able to produce a reduction in caspase-3 mRNA and activated caspase-3 protein was higher than that at which measurable increases in cell viability were seen, suggesting that caspase-3 may be only one of several targets involved in minocycline-mediated retinal cell neuroprotection. Caspase-independent pathways leading to apoptosis may include the mitochondrial release of apoptosis inducing factor or endonuclease G (Cao et al., 2003). Furthermore, minocycline has also been reported to block caspase-independent death triggered by etoposide in striatal neurons (Wang et al., 2003).

Minocycline has recently been shown to significantly reduce 6-hydroxydopamine-induced production of reactive oxygen species in cerebellar granule neurons (Lin et al., 2003). Excitotoxicity leads to mitochondrial instability and increased production of reactive oxygen species; thus, the neuroprotective effects of minocycline in retinal cell excitotoxicity may involve antioxidant properties.

In conclusion, this report extends previous observations on the actions of minocycline as a neuroprotectant. First, we demonstrated that minocycline, but not tetracycline, can function as a neuroprotective compound in retinal cell culture models. Second, our results indicate that the retinal neuroprotective actions of minocycline occur via mechanisms that are independent of NMDARs and glutamate-dependent Ca^{2+} influx but result in inhibition of caspase-3 and probably additional caspase-3-independent pathways. Last, our data demonstrate that the actions of minocycline in neuronal cultures do not require non-neuronal cells, because minocycline was able to effectively protect PC-12 cells in the absence of glia. Together, these results provide the rationale for further investigation of minocycline as a possible therapeutic agent for degenerative diseases of retina and optic nerve.

Acknowledgments

We acknowledge the technical assistance of Xiaoying (Alicia) Jia, Kelly Stevens, and Terry Levatte.

References

Baptiste DC, Hartwick AT, Jollimore CA, Baldridge WH, Chauhan BC, Tremblay F, and Kelly ME (2002) Comparison of the neuroprotective effects of adrenoceptor drugs in retinal cell culture and intact retina. *Investig Ophthalmol Vis Sci* **43:** 2666–2676.

Barber AJ, Nakamura M, Wolpert EB, Reiter CE, Seigel GM, Antonetti DA, and Gardner TW (2001) Insulin rescues retinal neurons from apoptosis by a phosphatidylinositol 3-kinase/Akt-mediated mechanism that reduces the activation of caspase-3. *J Biol Chem* **276:**32814–32821.

Bertolesi GE, Shi C, Elbaum L, Jollimore C, Rozenberg G, Barnes S, and Kelly ME (2002) The Ca^{2+} channel antagonists mibefradil and pimozide inhibit cell growth via different cytotoxic mechanisms. *Mol Pharmacol* **62:**210–219.

Boniece I and Wagner JA (1993) Growth factors protect PC-12 cells against ischemia by a mechanism that is independent of PKA, PKC and protein synthesis. *J Neurosci* **13:**4220–4228.

Cao G, Clark RS, Pei W, Yin W, Zhang F, Sun FY, Graham SH, and Chen J (2003) Translocation of apoptosis-inducing factor in vulnerable neurons after transient

cerebral ischemia and in neuronal cultures after oxygen-glucose deprivation. *J Cereb Blood Flow Metab* **23:**1137–1150.
Chen M, Ona VO, Li M, Ferrante RJ, Fink KB, Zhu S, Bian J, Guo L, Farrell LA, Hersch SM, et al. (2000) Minocycline inhibits caspase-1 and caspase-3 expression and delays mortality in a transgenic mouse model of Huntington disease. *Nat Med* **6:**797–801.
Friedlander RM (2003) Apoptosis and caspases in neurodegenerative diseases. *N Engl J Med* **348:**1365–1375.
Giuliano M, Lauricella M, Vassallo E, Carabillo M, Vento R, and Tesoriere G (1998) Induction of apoptosis in human retinoblastoma cells by topoisomerase inhibitors. *Investig Ophthalmol Vis Sci* **39:**1300–1311.
Greene LA (1978) Nerve growth factor prevents the death and stimulates the neuronal differentiation of clonal PC-12 pheochromocytoma cells in serum-free medium. *J Cell Biol* **78:**747–755.
Harrison DC, Davis RP, Bond BC, Campbell CA, James MF, Parsons AA, and Philpott KL (2001) Caspase mRNA expression in a rat model of focal cerebral ischemia. *Brain Res Mol Brain Res* **89:**133–146.
Hirooka K, Bertolesi GE, Kelly ME, Denovan-Wright EM, Sun X, Hamid J, Zamponi GW, Juhasz AE, Haynes LW, and Barnes S (2002) T-Type calcium channel alpha1G and alpha1H subunits in human retinoblastoma cells and their loss after differentiation. *J Neurophysiol* **88:**196–205.
Hughes EH, Schlictenbrede FC, Murphy CC, Broderick C, van Rooijen N, Ali RR, and Dick D (2004) Minocycline delays photoreceptor death in the rds mouse through a microglia-independent mechanism. *Exp Eye Res* **78:**1077–1084.
Johnson JW and Ascher P (1987) Glycine potentiates the NMDA response in cultured mouse brain neurons. *Nature (Lond)* **325:**529–531.
Kermer P, Klocker N, Labes M, and Bahr M (1998) Inhibition of CPP32-like proteases rescues axotomized retinal ganglion cells from secondary cell death in vivo. *J Neurosci* **18:**4656–4662.
Kriz J, Nguyen MD, and Julien JP (2002) Minocycline slows disease progression in a mouse model of amyotrophic lateral sclerosis. *Neurobiol Dis* **10:**268–278.
Lacomblez L, Bensimon G, Leigh PN, Guillet P, and Meininger V (1996) Dose-ranging study of riluzole in amyotrophic lateral sclerosis. *Lancet* **347:**1425–1431.
Lambeng N, Michel PP, Brugg B, Agid Y, and Ruberg M (1999) Mechanisms of apoptosis in PC-12 cells irreversibly differentiated with nerve growth factor and cyclic AMP. *Brain Res* **821:**60–68.
Lambeng N, Willaime-Morawek S, Mariani J, Ruberg M, and Brugg B (2003) Activation of mitogen-activated protein kinase pathways during the death of PC-12 cells is dependent on the state of differentiation. *Brain Res Mol Brain Res* **111:**52–60.
Larner AJ (2000) Neuronal apoptosis as a therapeutic target in neurodegenerative disease. *Exp Opin Ther Patent* **10:**1493–1518.
Liberatore GT, Jackson-Lewis V, Vukosavic S, Mandir AS, Vila M, McAuliffe WG, Dawson VL, Dawson TM, and Przedborski S (1999) Inducible nitric oxide synthase stimulates dopaminergic neurodegeneration in the MPTP model of Parkinson disease. *Nat Med* **5:**1403–1409.
Lin S, Wei X, Xu Y, Yan C, Dodel R, Zhang Y, Liu J, Klaunig JE, Farlow M, and Du Y (2003) Minocycline blocks 6-hydroxydopamine-induced neurotoxicity and free radical production in rat cerebellar granule neurons. *Life Sci* **72:**1635–1641.
Liu B and Hong JS (2003) Role of microglia in inflammation-mediated neurodegenerative diseases: mechanisms and strategies for therapeutic intervention. *J Pharmacol Exp Ther* **304:**1–7.
McKinnon SJ (2003) Glaucoma: ocular Alzheimer's disease? *Front Biosci* **8:**s1140–s1156.
Osborne NN, Ugarte M, Chao M, Chidlow G, Bae JH, Wood JP, and Nash MS (1999) Neuroprotection in relation to retinal ischemia and relevance to glaucoma. *Surv Ophthalmol* **43 (Suppl 1):**S102–128.
Pellegrini JW and Lipton SA (1993) Delayed administration of memantine prevents *N*-methyl-D-aspartate receptor-mediated neurotoxicity. *Ann Neurol* **33:**403–407.
Quigley HA (1999) Neuronal death in glaucoma. *Prog Retinal Eye Res* **18:**39–57.
Reisberg B, Doody R, Stöffler A, Schmitt F, Ferris S, and Möbius HJ (2003) Memantine in moderate-to-severe Alzheimer's disease. *N Engl J Med* **348:**1333–1341.
Scarabelli TM, Stephanou A, Pasini E, Gitti G, Townsend P, Lawrence K, Chen-Scarabelli C, Saravolatz L, Latchman D, Knight R, et al. (2004) Minocycline inhibits caspase activation and reactivation, increases the ratio of XIAP to Smac/DIABLO and reduces the mitochondrial leakage of cytochrome C and Smac/DIABLO. *J Am Coll Cardiol* **43:**865–875.
Schulz JB, Weller M, Matthews RT, Heneka MT, Groscurth P, Martinou JC, Lommatzsch J, von Coelln R, Wullner U, Loschmann PA, et al. (1998) Extended therapeutic window for caspase inhibition and synergy with MK-801 in the treatment of cerebral histotoxic hypoxia. *Cell Death Diff* **5:**847–857.
Seigel GM (1996) Establishment of an E1A-immortalized retinal cell culture. *In Vitro Cell Dev Biol Anim* **32:**66–68.
Seigel GM, Chiu L, and Paxhia A (2000) Inhibition of neuroretinal cell death by insulin-like growth factor-1 and its analogs. *Mol Vis* **6:**157–163
Seigel GM, Takahashi M, Adamus G, and McDaniel T (1998) Intraocular transplantation of E1A-immortalized retinal precursor cells. *Cell Transplant* **7:**559–566.
Sun W, Seigel GM, and Salvi RJ (2002) Retinal precursor cells express functional ionotropic glutamate and GABA receptors. *Neuroreport* **13:**2421–2424.
Tahzib NG, Ransom NL, Reitsamer HA, and McKinnon SJ (2004) Alpha-fodrin is cleaved by caspase-3 in chronic ocular hypertensive (COH) rat model of glaucoma. *Brain Res Bull* **62:**491–495.
Tezel G and Wax MB (1999) Inhibition of caspase activity in retinal cell apoptosis induced by various stimuli in vitro. *Investig Ophthalmol Vis Sci* **40:**2660–2667.
Tikka T, Fiebich BL, Goldsteins G, Keinanen R, and Koistinaho J (2001) Minocycline, a tetracycline derivative, is neuroprotective against excitotoxicity by inhibiting activation and proliferation of microglia. *J Neurosci* **21:**2580–2588.
Tikka TM and Koistinaho JE (2001) Minocycline provides neuroprotection against *N*-methyl-D-aspartate neurotoxicity by inhibiting microglia. *J Immunol* **166:**7527–7533.
Vaghefi H, Hughes AL, and Neet KE (2004) Nerve growth factor withdrawal-mediated apoptosis in naive and differentiated PC-12 cells through p53/caspase-3-dependent and -independent pathways. *J Biol Chem* **279:**15604–15614.
Wang X, Zhu S, Drozda M, Zhang W, Stavrovskaya IG, Cattaneo E, Ferrante RJ, Kristal BS, and Friedlander RM (2003) Minocycline inhibits caspase-independent and -dependent mitochondrial cell death pathways in models of Huntington's disease. *Proc Natl Acad Sci USA* **100:**10483–10487.
Weinreb RN and Levin LA (1999) Is neuroprotection a viable therapy for glaucoma? *Arch Ophthalmol* **117:**1540–1544.
Weinreb O, Bar-Am O, Amit T, Chillag-Talmor O, and Youdim MB (2004) Neuroprotection via pro-survival protein kinase C isoforms associated with Bcl-2 family members. *FASEB J* **18:**1471–1473.
Whyte P, Ruley H, and Harlow E (1988) Two regions of the adenovirus early region 1A proteins are required for transformation. *J Virol* **62:**257–265.
Wirtz-Brugger F and Giovanni A (2000) Guanosine 3′,5′-cyclic monophosphate mediated inhibition of cell death induced by nerve growth factor withdrawal and beta-amyloid: protective effects of propentofylline. *Neuroscience* **99:**737–750.
Wu DC, Jackson-Lewis V, Vila M, Tieu K, Teismann P, Vadseth C, Choi DK, Ischiropoulos H, and Przedborski S (2002) Blockade of microglial activation is neuroprotective in the 1-methyl-4-phenyl-1,2,3,6-tetrahydropyridine mouse model of Parkinson disease. *J Neurosci* **22:**1763–1771.
Yang L, Sugama S, Chirichigno JW, et al. Gregorio J, Lorenzl S, Shin DH, Browne SE, Shimizu Y, Joh TH, Beal MF, et al. (2003) Minocycline enhances MPTP toxicity to dopaminergic neurons. *J Neurosic Res* **74:**278–285.
Yrjänheikki J, Keinänen R, Pellikka M, Hökfelt T, and Koistinaho J (1998) Tetracyclines inhibit microglial activation and are neuroprotective in global brain ischemia. *Proc Natl Acad Sci USA* **95:**15769–15774.
Yrjänheikki J, Tikka T, Keinänen R, Goldsteins G, Chan PH, and Koistinaho J (1999) A tetracycline derivative, minocycline, reduces inflammation and protects against focal cerebral ischemia with a wide therapeutic window. *Proc Natl Acad Sci USA* **96:**13496–13500.
Zhu S, Stavrovskaya IG, Drozda M, Kim BY, Ona V, Li M, Sarang S, Liu AS, Hartley DM, Wu du C, et al. (2002) Minocycline inhibits cytochrome c release and delays progression of amyotrophic lateral sclerosis in mice. *Nature (Lond)* **417:**74–78.

Address correspondence to: Dr. Melanie Kelly, Department of Pharmacology, Dalhousie University, Halifax, Nova Scotia, Canada, B3H 4H7. E-mail: melanie.kelly@dal.ca